

PARAMETRIC IDEAL CYCLE ANALYSIS
OF A SCRAMJET ENGINE
AT A CONSTANT COMBUSTION MACH NUMBER

An Undergraduate Honors Thesis Project
presented to the MAE Honors Committee
at the University of Missouri - Columbia

In Fulfillment
of the Requirements for the Class
Undergraduate Honors Research

by

JANA MOORE

Dr. Craig Kluever, Thesis Supervisor

DECEMBER 2016

The undersigned have examined the undergraduate honors research project entitled

PARAMETRIC IDEAL CYCLE ANALYSIS OF A SCRAMJET ENGINE

Presented by Jana Moore

A candidate for the degree Bachelor of Science in Mechanical Engineering

And hereby certify that in their opinion it is worthy of acceptance

Dr. Craig A. Kluever

Dr. Ming Xin

ACKNOWLEDGEMENTS

I would like to thank Professor Craig Kluever for his willingness to advise me and guide me through the process selecting a research topic and submitting an undergraduate honors research project. He allowed me the freedom to work independently but was always quick to respond to my queries and made himself readily available to meet when my questions required more discussion than could be handled in email correspondence.

Special thanks also goes to Professor J.A. Roux of the University of Mississippi for taking the time to speak with me about his research on the ideal scramjet engine cycle. His clarifications regarding constant combustion Mach number versus constant combustion velocity as well as his explanation of thrust flux are the cornerstones of this project.

Finally, I must thank my friends and family who believed a public school music teacher could become a mechanical engineer and the Scholastic Weekly Reader for inspiring a 10 year old girl.



Note: This image is a scan of the October 12th, 1984 article from the Scholastic Weekly Reader which is how I found out that Christie McAuliffe was selected to be an astronaut and is still in my childhood scrapbook.

TABLE OF CONTENTS

ACKNOWLEDGEMENTS	ii
LIST OF TABLES	iv
LIST OF FIGURES	v
ABSTRACT	1
INTRODUCTION	2
Background	2
Thesis Overview	4
LITERATURE REVIEW	6
PROCEDURE	9
Specific Thrust	11
Fuel-to-Air Mass Flow Ratio	15
Thrust Specific Fuel Consumption	18
Thrust Flux	18
Efficiencies	21
<i>Thermal Efficiency</i>	21
<i>Propulsive Efficiency</i>	23
<i>Overall Efficiency</i>	25
RESULTS	26
Parametric Studies Modeling Ramjet Maximum Temperature Limits	28
Parametric Studies Modeling Material Temperature Limits When $M_c < M_0$ or $M_c \geq M_0$	32
CONCLUSION	37
REFERENCES	39
APPENDICES	41
1. Flight conditions at 12,000 m for constant combustion Mach numbers	41
2. Flight conditions at 12,000 m for constant combustion Mach numbers where $\tau_\lambda = T'_{\max}/T_0$ for $M_c < M_0$ or $\tau_\lambda = T''_{\max}/T_0$ for $M_c < M_0$	42
3. Flight conditions at 20,000 m for constant combustion Mach numbers where $\tau_\lambda = T'_{\max}/T_0$ for $M_c < M_0$ or $\tau_\lambda = T''_{\max}/T_0$ for $M_c < M_0$	43
4. Flight conditions at 30,000 m for constant combustion Mach numbers where $\tau_\lambda = T'_{\max}/T_0$ for $M_c < M_0$ or $\tau_\lambda = T''_{\max}/T_0$ for $M_c < M_0$	44

LIST OF TABLES

Table 1. Selected inputs for an ideal scramjet engine cycle	10
Table 2. Ideal ambient conditions at an altitude of 12 km.....	10
Table 3. Results of ideal scramjet cycle analysis parameters for a freestream Mach number of 6 and a combustion Mach number of 2 at an altitude of 12 km.	26
Table 4. Comparison of parametric measures at an altitude of 12 km for a ramjet with $M_c = 0$ and a scramjet with $M_c=2$	27
Table 5. Parameters for light conditions at 12,000 m.....	41
Table 6. Material temperature limit conditions at 30,000 m.....	41
Table 7. Material temperature limit conditions at 12,000 m when $M_c < M_0$	42
Table 8. Combustion Chamber entrance conditions at 12,000 m.....	42
Table 9. Thrust Flux variables at 12,000 m	42
Table 10. Parameters for light conditions at 20,000 m.....	43
Table 11. Material temperature limit conditions at 20,000 m when $M_c < M_0$	43
Table 12. Combustion Chamber entrance conditions at 20,000 m.....	43
Table 13. Thrust flux variables at 20,000 m	44
Table 14. Parameters for light conditions at 30,000 m.....	44
Table 15. Material temperature limit conditions at 30,000 m when $M_c < M_0$	44
Table 16. Combustion Chamber entrance conditions at 30,000 m.....	45
Table 17. Thrust Flux variables at 30,000 m	45

LIST OF FIGURES

Fig. 1. Scramjet engine diagram.	4
Fig. 2. Specific thrust vs freestream Mach Number of a scramjet at an altitude of 12 km as compared to a ramjet with an internal combustion $M_c = 0$	28
Fig. 3. Fuel-to-air mass flow ratio vs freestream Mach number of a scramjet at an altitude of 12 km as compared to a ramjet with an internal combustion $M_c = 0$	29
Fig. 4. Thrust specific fuel consumption vs Mach number of a scramjet at an altitude of 12 km as compared to a ramjet with an internal combustion $M_c = 0$	29
Fig. 5. Thermal efficiency vs freestream Mach number of a scramjet at an altitude of 12 km as compared to a ramjet with an internal combustion $M_c = 0$	30
Fig. 6. Propulsive efficiency vs freestream Mach number of a scramjet at an altitude of 12 km as compared to a ramjet with an internal combustion $M_c = 0$	31
Fig. 7. Overall Efficiency vs Freestream Mach Number of a scramjet at an altitude of 12 km as compared to a ramjet with an internal combustion $M_c = 0$	31
Fig. 8. Modified specific thrust vs freestream Mach number of a scramjet at an altitude of 12 km as compared to a ramjet with an internal combustion $M_c = 0$	32
Fig. 9. Modified fuel-to-Air mass flow ratio vs freestream Mach number of a scramjet at an altitude of 12 km as compared to a ramjet with an internal combustion $M_c = 0$	33
Fig. 10. Modified Thrust-Specific Fuel Consumption vs Mach Number of a scramjet at an altitude of 12 km as compared to a ramjet with an internal combustion $M_c = 0$	34
Fig. 11. Modified thrust-specific fuel consumption vs Mach number at constant combustion Mach 2 over a range of altitudes	34
Fig. 12. Thrust flux vs Freestream Mach number of a scramjet at an altitude of 12 km	35
Fig. 13. Thrust flux vs freestream Mach number at constant combustion Mach 2.....	35
Fig. 14. Modified thermal efficiency vs freestream Mach number of a scramjet at an altitude of 12 km as compared to a ramjet with an internal combustion $M_c = 0$	36
Fig. 15. Modified Propulsive Efficiency vs Freestream Mach Number of a scramjet at an altitude of 12 km as compared to a ramjet with an internal combustion $M_c = 0$	36

Fig. 16. Modified Overall Efficiency vs Freestream Mach Number of a scramjet at an altitude of 12 km as compared to a ramjet with an internal combustion $M_c = 0$ 37

ABSTRACT

The 1920's and 1930's saw the development of the turbojet engine and turbofan engine, respectively. Supersonic combustion ramjet or scramjet engine development began in the United States the early 1950's after the development of the ramjet engine in the late 1940's. However, unlike the research completed on the ideal cycle engine analysis for turbofans and turbojets little analysis has been published on the ideal scramjet engine cycle.

Employing isentropic assumptions of the Brayton Cycle, this research project will examine the published literature on the ideal cycle for the scramjet engine including six parametric measures common to the ideal engine cycle analysis for turbojets and turbofans; specific thrust, fuel-to-air mass flow ratio, thrust specific fuel consumption, thermal, propulsive, and overall all efficiencies as well as a seventh parameter, thrust flux, across a range of freestream Mach numbers at various constant combustion Mach numbers and altitudes. By design, a ramjet engine's combustion Mach number is approximately zero thus some discussion and comparison of a ramjet ideal engine cycle will be included. Additionally, a qualitative discussion of the losses creating a non-ideal engine cycle will be discussed. Finally, due to the supersonic speed of the flow inside the combustion chamber discussion regarding constant Mach versus constant velocity will be examined.

At the conclusion of this project the reader should come away with a better understanding of why a constant combustion velocity is a more practical model for the burner due to the pressure losses in the combustor. Additionally, it will also be shown that the new, seventh parametric measure, thrust flux, is a better indicator of at what flight Mach number the scramjet engine thrust will peak rather than the formerly assumed parametric measure, thrust specific fuel consumption.

INTRODUCTION

Background

The concept of the ramjet and subsequently the scramjet has been explored by the countries of the world since the early 20th century. French engineer, René Leduc, is credited with the first ramjet design in the 1920's and the patent in 1934. As Leduc began to realize his design in the mid 1940's Germany, the former USSR, and the United States were developing experimental ramjets and scramjets. In a race to achieve supersonic flight, post-World War II nations saw the first test glide-flights of ramjets including Leduc's ramjet design in 1946 (Segal 2009). The first manned supersonic flight, accredited to U.S. Airforce officer and test pilot, Chuck Yeager, soon followed in 1947. In 1958 researchers Weber and McKay helped advance our understanding of combustion by stating that, "...combustion can take place in supersonic airflows without creating considerable losses through shock-wave generation," and that, "efficiencies increase with speed in the range of Mach 4-7," for both ramjets and scramjets. Weber and McKay also supposed that the scramjet efficiencies could be increased at higher Mach numbers with the right diffuser design (Segal 2009).

In the United States during the 1960's NASA both worked on a Hypersonic Research Engine (HRE) program with the goal of building and testing hypersonic flight ramjet and scramjet engines by altering the X-15A-2 engine to hold hydrogen fuel for the scramjet as well as a joint effort with the U.S Air Force to further pursue scramjet engineering. By this time the Australian and Japanese researchers had also entered the ramjet/scramjet research race. As more countries began to contribute to scramjet research more was becoming known about the efficiencies of fuel mixing and engine design. In the 1990's several collaborative test flights between NASA and Moscow researchers were conducted with axisymmetric scramjet engines.

Research showed that, “The swept inlet cowl provided a flow stability of a large flight regime, and fuel-injected modulation from the struts allows operation over a broad Mach number range with a fixed geometry” (Segal 2009). “But while these applications have all been for short durations, or while decelerating, the current focus on hypersonic flight,” and thus supersonic flight, “is aimed at sustained flight using engines that burn fuel with oxygen from the atmosphere” (Lewis 2010).

As of 2001, considerable work has been done by the University Queensland in Australia to expand our understanding of supersonic flight with their HyShot program. In 2002 experiments with an axisymmetric HyShot II provided flight data at approximated Mach 7.5 flight conditions comparable with ground testing results which, “...confirmed the presence of supersonic combustion during the approximately 3 s test window at altitudes between 35 and 29 km” (Smart, Hass and Paull 2006).

In the United States the Pratt & Whitney Rocketdyne SJX61 engine completed successful ground tests simulating Mach 5 flight conditions at NASA’s Langley Research Center in 2008. In May of 2010 the SJX61 was installed on Boeing’s X-51A which was then mounted under a B-52 bomber as a part of the continued collaborative relationship between the U.S. Air force and NASA. Once up to the desired altitude of 50,000 ft and speed of Mach 5 the X-51A was released from the bomber and switched to hydrocarbon JP-7 fuel which generated enough uphill acceleration for 200 seconds. Though considered a successful flight at 200 s barriers to longer, sustained flight such as exceeding material temperature limits for aircraft at supersonic speeds continue to be a challenge for researchers. Thus, as research continues, this project will be a review of the most recent literature and will attempt to present the reader with a simple, plausible scramjet ideal engine cycle analysis.

Thesis Overview

The basic components of a ramjet engine are simple to understand. Comprised of an inlet (or diffuser), a combustion chamber (or burner), and an exit nozzle the ramjet engine is an air-breathing engine that flies at supersonic speeds.

Because the airflow is compressed by “ramming” into the diffuser (inlet) and decelerated entering the combustion chamber (burner) there is no need for moving engine parts. Rather the flow is decelerated to subsonic speeds by the geometry of the inlet resulting in a highly compressed airflow which is then injecting the fuel and ignited in the combustion chamber. A supersonic combustion ramjet, SCRJ or scramjet shown in Fig. 1, as it is commonly referred to, differs slightly from a ramjet in that the flow remains at supersonic speeds as it is ignited. Exiting the combustion chamber, the expansion of the flow as it exits the nozzle provides the available thrust.

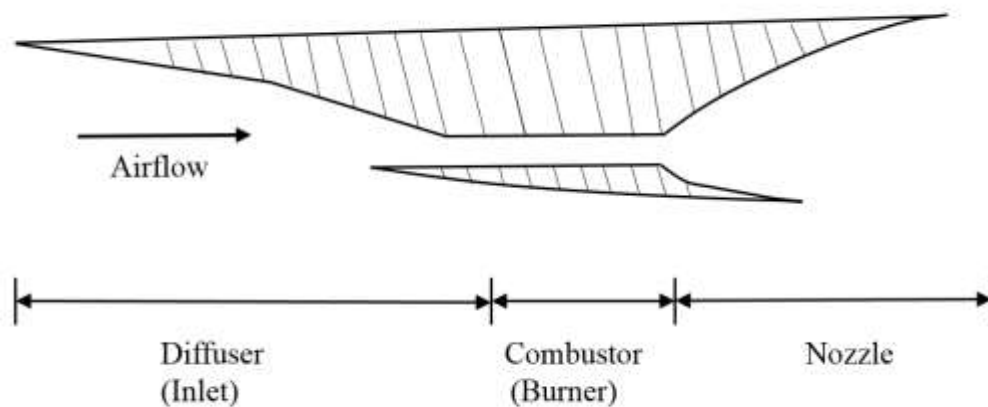


Fig. 1. Scramjet engine diagram.

The lack of moving engine parts, however, makes the modeling of equations for an ideal engine cycle analysis deceptively complex due to the limited understanding of airflow behavior at supersonic speeds.

One professor from the University of Mississippi, Dr. J.A. Roux, attempted to provide a simple set of algebraic equations based in part on the ideal turbofan, turbojet, and ramjet engine cycle analysis and summarize them into a technical note published in the *Journal of Thermophysics and Heat Transfer*. For this project an examination of Roux's publication in which he presented his first attempt at a parametric study of an ideal scramjet cycle analysis was conducted by modeling the equations within the technical note and attempting to replicate the results for the six parametric studies. It is important to note that in these studies it was assumed that the total maximum temperature of the flow was experienced inside the engine. Supporting literature was reviewed to confirm the accuracy of the modeling equations which led to the discovery of a revised technical note by Roux. In his revised ideal cycle analysis he attempted to model flow behavior where depending whether the combustion Mach number less than or greater than the freestream Mach number determined whether the total temperature limit was experienced inside or outside the engine. He also identified a seventh parameter which he named thrust flux and which showed a potential for peak thrust at Mach speeds much higher than previously assumed. With the results of Roux's parametric studies for reference, a further examination was conducted of the thrust-specific fuel consumption and thrust flux. Altitude was varied at a constant combustion Mach number and compared to similar figures where the combustion Mach number was varied to see which variable is more impactful on performance. Results will show that thrust-specific fuel consumption increases as combustion Mach number increases and that altitude has little effect on the parameter. Additionally, thrust flux increases as combustion Mach number increases and decreases as altitude increases which leads to the conclusion that a high combustion Mach number is the more impactful of the two variables when examining peak thrust performance.

LITERATURE REVIEW

A search of the literature uncovered multiple technical notes by University of Mississippi professor, J.A. Roux. In his first technical note on the subject of the ideal scramjet engine cycle analysis, "Parametric Ideal Scramjet Cycle Analysis" published in 2011, Roux acknowledges that there is readily available "well know and documented" cycle analysis of the ideal turbofan and turbojet engines as well as the ideal ramjet engine (J. Roux 2011).

To create the foundation of his parametric study, Roux references the ideal engine cycle analysis of the ramjet found in the textbook written by Mattingly and Ohain in 2006 as well as a 1992 textbook by Hill and Peterson to analyze an equivalent ideal scramjet engine cycle. In this article, Roux proposes to analyze the scramjet engine cycle as a variation of the ramjet engine referenced in the previously mentioned text but with supersonic combustion. The first half of the article is used to mathematically describe six performance measures including specific thrust, thrust-specific fuel consumption, fuel-to-air ratio, and thermal, propulsive, and overall efficiencies. The remaining article examines the results of the parametric performances over a range of freestream Mach numbers and compares how the performances differs from a ramjet engine.

For analysis of the scramjet engine, "isentropic inlet process, a constant pressure combustion process, and isentropic nozzle process, and a constant pressure heat rejection process where the nozzle exit static pressure is equal to the freestream flight ambient static pressure" (J. Roux 2011) assumptions of the Brayton cycle were modeled using the text on the ramjet engine from Mattingly and Ohain as well as a 1998 textbook by Cengel and Boles on the scramjet engine process. Complete scramjet cycle analysis is reviewed using the text from a 2006 paper presented at the 25th International Congress of the Aeronautical Sciences by Erik Prisell and the

2009 text of C. Segal's book "The Scramjet Engine, Processes, and Characteristics." Roux expands on his previous work with a discussion of the graphical results over various internal combustion Mach numbers. Most notably Roux concludes that the form of the ideal cycle equations for a scramjet is the same as a ramjet except the material temperature limit, τ_λ . "The same maximum materials limit temperature T_{max} is experienced by the engine material, but in the scramjet engine the total gas temperature, T'_{max} never affects the engine material. The scramjet can achieve a significantly great total temperature, and therefore greater work as a result of this operation" (J. Roux 2011).

In 2013 Roux revises his parametric ideal scramjet cycle analysis for the fuel-to-air ratio, f , to account for a total maximum temperature when the combustion Mach number is less than the flight Mach number or for when the combustion Mach number is greater than the flight Mach number. He also includes a seventh parameter he has named thrust flux which is a ratio of the thrust, F , to the diffuser (engine inlet) exit area; burner entrance area, A_2 . The most significant result from the addition of a seventh parameter is the discovery of a peak in thrust at a flight Mach number much higher than previously estimated with specific thrust at the same flight Mach number.

In 2015 researchers from the Harbin Institute of Technology published comments on Roux's previous work regarding ideal scramjet cycle analysis. In their paper the researchers stated that, "...assumptions of heat addition occurring at both constant static pressure and constant combustion Mach number, which imply a constant total pressure across the burner, are obviously unjustified for a scramjet." Even a supersonic combustion Mach number as low as two "...may cause more than a 40% reduction in total pressure" (Yang, et al. 2015). Rather, researchers stated that an examination of the Brayton cycle for the constant static pressure heat

rejection process yields a constant velocity across the burner rather than a constant Mach number. Therefore, "...under the assumption of heat addition occurring at constant static pressure, the total pressure loss must be taken into consideration when analyzing the combustion process in the scramjet..." thus "Without the assumption of a constant combustion Mach number, it is achievable and more accurate to provide the parametric representation of the performance parameters for the ideal scramjet" (Yang, et al. 2015). Roux replied in the same year that though their comments regarding the constant static pressure head addition process had merit and was worth review it "...*may or may* not yield a simple parametric description of scramjet propulsion..." Roux went to state that, to date, his revised parametric scramjet analysis his paper had "...the only known simple scramjet cycle parametric description *with demonstrated results* for the seven engine performance parameters" (J. Roux 2015).

The most recent published work by J.A. Roux in the summer of 2016 is a follow up to the comments and reply of his previous work on the ideal scramjet engine cycle. Based on the Brayton cycle, his previous work model equations assuming a constant combustion Mach number while maintaining a constant static pressures during the combustion process. In this latest published work, rather than assuming a constant Mach number through the combustion chamber he recalculates the seven previously discussed parameters with a complete model of constant velocity through the combustion chamber. To complete the modeling of equations, results of the paper revealed that in order to assume a constant Mach number or constant velocity you cannot have a constant cross-section area of the combustor. Then once calculated Roux compares the graphical results of the constant Mach number versus the same parameters at constant velocity. What is revealed is that the graphical peaks for specific thrust, thrust specific fuel consumption, and thrust flux occur at the same flight Mach numbers for both constant

velocity and constant Mach number but the magnitude is much lower for constant velocity than it is for constant Mach. From these results the author notes that though the performance at a contact Mach number is better than at constant velocity through the combustor though it may not be realistic due to an anticipated decrease in total pressure.

PROCEDURE

For an ideal engine cycle analysis, a calorically perfect gas is assumed such that the ratio of specific heats, γ , is constant and therefore the specific heat at a constant pressure, c_p , remains constant. Additionally, it was assumed that the fuel mass-flow rate, \dot{m}_{fuel} , is so small as compared to the mass-flow rate of the free stream air, \dot{m}_0 , that \dot{m}_{fuel} could be neglected. In other words, the mass introduced by the addition of the fuel is negligible therefore the mass flow rate at the exit, \dot{m}_9 is approximately equal to the mass flow rate of the freestream \dot{m}_0 .

From the Brayton cycle, adiabatic and frictionless conditions, also known as isentropic flow, are assumed from the freestream before the engine through the inlet and through the nozzle to the exit. Additionally, constant stagnation pressure is assumed through the combustion chamber and the nozzle exit static pressure is equal to the ambient static pressure.

With assumptions defined, inputs and flight conditions needed to be identified to calculate the ideal cycle analysis. The values chosen were those for the freestream and combustion Mach numbers of $M_0 = 6$ and $M_c = 2$, respectively. Additionally, figures such as fuel lower heating, h_{PR} , and material temperature limit, T_{max} were selected and are shown in Table 1.

Table 1. Selected inputs for an ideal scramjet engine cycle

Selected Input	Value	Units
M_0 , Freestream Mach number	6	-
M_c , Combustion Mach number	2	-
h_{PR} , Fuel lower heating value	42,800	kJ/kg
T_{max} , Material temperature limit	1600	K

Finally, based on a flight altitude of 12 km values such as ambient temperature, T_0 , speed of sound, a_0 , atmospheric pressure, P_0 , ratio of specific heats, γ , and specific heat at a constant pressure, c_p , could be identified and listed in Table 2.

Table 2. Ideal ambient conditions at an altitude of 12 km

Atmospheric Conditions	Value	Units
h , Altitude	12	km
T_0 , Ambient Temperature	217	K
a_0 , Speed of air	295.07	m/s
P_0 , Freestream static pressure	1.9403	N/cm ²
c_p , Specific heat at constant pressure	1.004	kJ/kg-K
γ , Ratio of specific heats	1.4	-
R , Universal gas constant	287	J/kg-K

Specific Thrust

With inputs selected the inlet temperature ratio, τ_r , in Eq. (1) can be easily calculated as a ratio of freestream total temperature T_{t0} to freestream ambient temperature T_0 .

$$\tau_r = T_{t0}/T_0 \quad (1)$$

where T_{t0} is the total freestream temperature.

$$T_{t0} = T_0 \left(\frac{\gamma-1}{2} M_0^2 \right) \quad (2)$$

Next the thrust equation, F , is calculated as a change in momentum with the change of time. The mass flow rate at the exit of the nozzle is \dot{m}_9 and the mass flow rate of the freestream is \dot{m}_0 . Additionally, V_9 , P_9 , and A_9 represent the velocity, static pressure, and area at the exit.

$$F = (\dot{m}_9 V_9 - \dot{m}_0 V_0) + A_9(P_9 - P_0) \quad (3)$$

Based on previous assumptions about the ambient and exit static pressures equaling each other and the exit flow rate approximately equaling the freestream mass flow rate the equations yields,

$$F = \dot{m}_0(V_9 - V_0) \quad (4)$$

By rearranging the thrust equation an expression for the first of the parametric measures, specific thrust, develops in Eq. (5),

$$\frac{F}{\dot{m}_0} = a_0 \left(\frac{V_9}{a_0} - M_0 \right) \quad (5)$$

where the speed of sound, a_0 , is defined as

$$a_0 \equiv \sqrt{\gamma R T_0} \quad (6)$$

and can be calculated as

$$a_0 = \frac{M_0}{V_0} \quad (7)$$

The focus is now turned towards the exit velocity, V_9 , such that a relationship between the exit Mach number, M_9 , and the freestream Mach number, M_0 , can be established.

From the Eq. (5), specific thrust, the ratio of exit velocity to ambient sound of speed is squared as shown in Eq. (8),

$$\left(\frac{V_9}{a_0}\right)^2 = \frac{a_9^2 M_9^2}{a_0^2} = \frac{\gamma_9 R_9 T_9 M_9^2}{\gamma_0 R_0 T_0} \quad (8)$$

which due to previously stated assumptions about γ and R reduces to

$$\left(\frac{V_9}{a_0}\right)^2 = \frac{T_9}{T_0} M_9^2 \quad (9)$$

Next attention is turned to total exit pressure, P_{t9} , for reasons that will become evident shortly.

First is to evaluate P_{t9} as a ratio of pressures multiplied by ambient static pressure as shown in Eq. (10).

$$P_{t9} = P_0 \frac{P_{t0}}{P_0} \frac{P_{t2}}{P_{t0}} \frac{P_{t4}}{P_{t2}} \frac{P_{t9}}{P_{t4}} = P_0 \pi_r \pi_d \pi_b \pi_n \quad (10)$$

However due to isentropic assumptions, the diffuser ratio, π_d , the burner ratio, π_b , and the nozzle ratio, π_n , are equal to 1 thus

$$P_{t9} = P_0 \pi_r \quad (11)$$

Additionally, due to previous stated assumptions about the static exit and ambient pressures the ratio of the exit stagnation pressure to the ambient pressure is defined the freestream pressure ratio seen in Eq. (12).

$$\frac{P_{t9}}{P_0} = \frac{P_{t9} P_0}{P_{t0} P_9} = \frac{P_0}{P_9} \pi_r = \pi_r \quad (12)$$

Returning to Eq. (9) the exit Mach number can be written using isentropic properties such that

$$M_9^2 = \frac{2}{\gamma-1} \left[\left(\frac{P_{t9}}{P_9} \right)^{(\gamma-1)/\gamma} - 1 \right] = \frac{2}{\gamma-1} \left(\pi_r^{(\gamma-1)/\gamma} - 1 \right) \quad (13)$$

Because the following relationship exists between pressure ratios and temperature ratios such that

$$\pi_r^{(\gamma-1)/\gamma} = \tau_r \quad (14)$$

the exit Mach number becomes

$$M_9^2 = \frac{2}{\gamma-1} (\tau_r - 1) = M_0^2 \quad (15)$$

In other words, the exit Mach number, M_9 , is equivalent to the ambient Mach number, M_0 .

Following the example of the total exit pressure, focus is now turned to the total exit temperature, T_{t9} , where

$$T_{t9} = T_0 \frac{T_{t0}}{T_0} \frac{T_{t2}}{T_{t0}} \frac{T_{t4}}{T_{t2}} \frac{T_{t9}}{T_{t4}} = T_0 \tau_r \tau_d \tau_b \tau_n \quad (16)$$

Again like the pressure ratios, due to isentropic assumptions, temperature ratios for the diffuser, τ_d , and the nozzle, τ_n , are equal to 1. However, due to the addition of heat in the burner the burner temperature ratio, τ_b , is not unity.

Thus the total exit temperature equation yields

$$T_{t9} = T_0 \tau_r \tau_b \quad (17)$$

Again since an isentropic relationship exists between stagnation-to-static pressure ratios and temperature ratios, the stagnation to static temperature ratio can be written as

$$\frac{T_{t9}}{T_0} = \left(\frac{P_{t9}}{P_9} \right)^{(\gamma-1)/\gamma} \quad (18)$$

Next Eq. (17) is divided by Eq. (18) resulting in a static temperature ratio seen in Eq. (19).

$$\frac{T_9}{T_0} = \frac{T_{t9}/T_0}{T_{t9}/T_9} = \frac{\tau_r \tau_b}{\left(\frac{P_{t9}}{P_9} \right)^{(\gamma-1)/\gamma}} = \frac{\tau_r \tau_b}{\tau_r} \quad (19)$$

Thus the burner temperature ratio can be represented by Eq. (20).

$$\frac{T_9}{T_0} = \tau_b \quad (20)$$

Now the exit velocity to speed of sound ratio can be rewritten in terms of the burner temperature ratio and ambient Mach number using Eqs. (15) and (20).

$$\left(\frac{V_9}{a_0} \right)^2 = \frac{T_9}{T_0} M_9^2 = \tau_b M_0^2 \quad (21)$$

Turing back to the expression previously developed for specific thrust in Eq. (5), algebraic substitutions using Eq. (21) now yield

$$\frac{F}{\dot{m}_0} = a_0 M_0 (\sqrt{\tau_b} - 1) \quad (22)$$

However it should be noted that the total material temperature limit to freestream temperature ratio can be developed as Eq. (23),

$$\tau_\lambda = \frac{c_p T_{max}}{c_p T_0} = \frac{T_{max}}{T_0} = \frac{T_{t2} T_{max}}{T_0 T_{t2}} = \tau_r \tau_b \quad (23)$$

thus the final form for specific thrust is

$$\frac{F}{\dot{m}_0} = a_0 M_0 \left(\sqrt{\frac{\tau_\lambda}{\tau_r}} - 1 \right) \quad (24)$$

Fuel-to-Air Mass Flow Ratio

The next parametric measure to develop is the fuel-to-air mass flow ratio which is defined as the ratio of the mass flow of the fuel to the mass flow of the air.

$$f \equiv \frac{\dot{m}_f}{\dot{m}_0} \quad (25)$$

Applying the steady flow energy equation to the control volume of the combustor gives

$$\dot{m}_0 h_{t2} + \dot{m}_f h_{PR} = (\dot{m}_0 + \dot{m}_f) h_{t4} \quad (26)$$

where h_{t2} and h_{t4} are the stagnation enthalpies entering and exiting the combustor which are defined as the product of the specific heat at a constant pressure, c_p , and stagnation temperature, T_t .

$$h_t = c_p T_t \quad (27)$$

Because of assumption previous stated about the mass flow rate and by substituting Eq. (27) into Eq. (24) the result yields Eq. (28),

$$\dot{m}_0 c_p T_{t2} + \dot{m}_f h_{PR} = \dot{m}_0 c_p T_{t4} \quad (28)$$

where T_{t2} is the total (or stagnation) temperature at the entrance of the burner and T_{t4} which equals T_{max} is the exit of the burner. By rearranging the Eq. (28) we develop the familiar format for the fuel-to-air mass flow ratio:

$$f = \frac{\dot{m}_f}{\dot{m}_0} = \frac{c_p T_{t2}}{h_{PR}} \left(\frac{T_{max}}{T_{t2}} - 1 \right) \quad (29)$$

where

$$T_{t0} = T_{t2} = T_0 \tau_r \quad (30)$$

and

$$T_{max}/T_{t2} = \tau_b \quad (31)$$

Substituting Eqs., (30) and (31) into (29) now yields

$$f = \frac{c_p T_0 \tau_r}{h_{PR}} (\tau_b - 1) \quad (32)$$

Recalling that

$$\tau_\lambda = \tau_r \tau_b \quad (33)$$

the parametric measure for the fuel-to-air mass flow ratio becomes,

$$f = \frac{c_p T_0}{h_{PR}} (\tau_\lambda - \tau_r) \quad (34)$$

Equation (34) is now in the form to be calculated for the second parametric measure.

It is at this point that the ideal cycle analysis for a ramjet and scramjet differ due to considerations of combustion Mach values. When the combustion Mach number is less than the freestream Mach number the total temperature to the freestream temperature ratio, τ_λ , becomes,

$$\tau_\lambda = \frac{T'_{max}}{T_0} \quad (35)$$

where T'_{max} is burner exit temperature shown in Eq. (35) such that the stagnation to static temperature ratio becomes dependent on the combustion Mach number shown in Eq. (36).

$$T'_{max} = T_{max} \left[1 + \frac{(\gamma-1)}{2} M_c^2 \right] \quad (36)$$

It should be noted that if M_c equaled zero the results would be for a ramjet. Next, when the combustion Mach number is greater than or equal to the freestream Mach number the total temperature to the freestream temperature ratio, τ_λ , becomes,

$$\tau_\lambda = \frac{T''_{max}}{T_0} \quad (37)$$

where T''_{max} is burner exit temperature shown in Eq. (37) such that the stagnation to static temperature ratio becomes dependent on the freestream Mach number shown in Eq. (38).

$$T''_{max} = T_{max} \left[1 + \frac{(\gamma-1)}{2} M_0^2 \right] \quad (38)$$

Thrust Specific Fuel Consumption

The third parametric measure in the ideal scramjet engine cycle analysis to be evaluated is developed from the ratio of the fuel-to-air mass flow to specific thrust, called thrust specific fuel consumption and is shown in Eq. (39).

$$S = \frac{f}{F/\dot{m}} \quad (39)$$

By simply substituting Eqs. (24) and (34) the thrust specific fuel consumption becomes,

$$S = \frac{c_p T_0 (\tau_\lambda - \tau_r)}{h_{PR} a_0 M_0 \left(\sqrt{\frac{\tau_\lambda}{\tau_r}} - 1 \right)} \quad (40)$$

Thrust Flux

The next parameter to develop is thrust flux. Thrust flux is dependent on the size of the flow areas and is comprised of the expression for specific thrust shown in Eq. (24) and mass flux where M_2 is the Mach number at the diffuser exit/burner entrance and is equivalent to M_c for a ramjet and a scramjet.

We begin with the general definition of mass-flow rate which is the product of the ambient density, ρ , velocity, V , and area, A .

$$\dot{m} = \rho AV \quad (41)$$

Noting the velocity can be expressed in terms of Mach number and airspeed, a , where

$$a = \sqrt{\gamma RT} \quad (42)$$

density can be written in terms of the ideal gas law

$$\rho = P/RT \quad (43)$$

and pressure can be written in terms of an isentropic relationship between static pressure, P , and total stagnation pressure, P_t , where T represents static temperature and T_t represents total stagnation temperature such that

$$P = P_t \left(\frac{T}{T_t} \right)^{\gamma/\gamma-1} \quad (44)$$

The mass-flow rate for an ideal compressible gas can now be expressed as

$$\dot{m} = \frac{AP_t}{\sqrt{T_t}} \sqrt{\frac{\gamma}{R}} M \left(1 + \frac{\gamma-1}{2} M^2 \right)^{-\gamma+1/2(\gamma-1)} \quad (45)$$

From the mass flow rate, Eq. (45), now a mass flow parameter, Γ , can be defined. When conditions are choked the Mach number is 1 and the area, A , is the throat area A^* our parameter which yields

$$\Gamma = \sqrt{\frac{\gamma}{R} \left(\frac{2}{\gamma+1} \right)^{\gamma+1/\gamma-1}} \quad (46)$$

Through substitution and algebraic manipulation Eq. (45) is transformed into

$$\Gamma = \frac{\dot{m}\sqrt{T_t}}{A^*P_t} \quad (47)$$

Next the mass flux is defined as the mass flow rate per the diffuser exit/burner entrance area, A_2 , such that

$$\frac{\dot{m}_0}{A_2} = \frac{\dot{m}_2}{A_2} = \frac{\dot{m}_0 A_2^*}{A_2^* A_2} = \frac{\dot{m}_2}{A_2^*} \left(\frac{A^*}{A} \right)_{M_2} \quad (48)$$

where by using Eq. (45) for the mass flux at the burner entrance and substituting Eq. (47) and (48) area yields

$$\frac{\dot{m}_2}{A_2^*} = \Gamma \frac{P_{t2}}{\sqrt{T_{t2}}} \quad (49)$$

Recalling isentropic assumptions for the Brayton cycle, the total stagnation temperature and pressure at the exit of the diffuser are equal to ambient conditions. Therefore stagnation-to-static relationships can be used to rewrite the ratio of total stagnation pressure at the diffuser exit/burner entrance to represent freestream conditions as

$$\frac{P_{t2}}{\sqrt{T_{t2}}} = \frac{P_{t0}}{\sqrt{T_{t0}}} = \frac{P_0}{\sqrt{T_0}} \frac{P_{t0}/P_0}{\sqrt{T_{t0}/T_0}} = \frac{P_0}{\sqrt{T_0}} \frac{(T_{t0}/T_0)^{\gamma/(\gamma-1)}}{\sqrt{T_{t0}/T_0}} \quad (50)$$

or

$$\frac{P_{t2}}{\sqrt{T_{t2}}} = \frac{P_0}{\sqrt{T_0}} \left(\frac{T_{t0}}{T_0} \right)^{\gamma/(\gamma-1)-1/2} = \frac{P_0}{\sqrt{T_0}} (\tau_r)^{(\gamma+1)/[2(\gamma-1)]} \quad (51)$$

Noting that γ is assumed to be 1.4, we now see that the exponent for τ_r equals 3 thus substituting Eqs. (49) and (51) into gives the mass flux expression

$$\frac{\dot{m}_0}{A_2} = \Gamma \left(\frac{A^*}{A} \right) \left(\frac{P_0}{\sqrt{T_0}} \right) \tau_r^3 \quad (52)$$

such that the area ratio is

$$\frac{A^*}{A} = \left\{ \frac{1}{M_2^2} \left[\frac{2}{(\gamma+1)} \left(1 + \frac{(\gamma-1)}{2} M_2^2 \right) \right]^{\gamma+1/\gamma-1} \right\}^{-1/2} \quad (53)$$

Combing Eq. (52) for mass flux, $\frac{\dot{m}}{A_2}$, with Eq. (24), for specific thrust, $\frac{F}{\dot{m}}$, finally yields the thrust flux in Eq. (54).

$$\frac{F}{A_2} = \left(\frac{F}{\dot{m}} \right) \left(\frac{\dot{m}}{A_2} \right) \quad (54)$$

Efficiencies

The final set of parameters to model for the ideal scramjet cycle analysis are the efficiencies which are very similar to those of the turbojet and turbofan efficiencies. The primary differences are based on temperature ratios that are not needed in the scramjet efficiencies such as compressor temperature ratio because the scramjet does not have a compressor.

Thermal Efficiency

Thermal efficiency is defined as the ratio of engine power output represented as the change in kinetic energy versus how much heat per fuel mass was added and indicates how effectively heat added to the air flow increases its energy. In other words, thermal efficiency can be represented as

$$\eta_{th} = \frac{P_{engine}}{\dot{m}_{fuel}h_{PR}} = \frac{\Delta KE}{\dot{m}_{fuel}h_{PR}} = \frac{\dot{m}_{in}(V_9^2/2 - V_0^2/2)}{\dot{m}_{fuel}h_{PR}} \quad (55)$$

where \dot{m}_{in} is the mass flow rate of the ambient air and the fuel, V_9 is the exit velocity, V_0 is the freestream velocity, and the engine power, P_{engine} is

$$P_{engine} = \dot{m}_{in} \frac{V_9^2}{2} - \dot{m}_{in} \frac{V_0^2}{2} \quad (56)$$

Through energy balance the denominator for Eq. (55) can be written as

$$\dot{m}_{fuel}h_{PR} = \dot{m}(h_{t4} - h_{t2}) \quad (57)$$

In the numerator the mass flow rate of the fuel as compared to the air is so small that it is neglected thus reduced to \dot{m} .

Noting that the total stagnation enthalpies for the ambient and exit velocities are Eqs. (58) and (59), respectively

$$h_{t9} = h_9 + \frac{V_9^2}{2} \quad (58)$$

$$h_{t0} = h_0 + \frac{V_0^2}{2} \quad (59)$$

the resulting substitutions of Eqs. (57-59) into (55) gives Eq. (60).

$$\eta_{th} = \frac{\dot{m}[(h_{t9}-h_9)-(h_{t0}-h_0)]}{\dot{m}(h_{t4}-h_{t2})} \quad (60)$$

By canceling the specific heats at constant pressure for all of the enthalpies and rearranging the fraction, a ratio of temperatures is revealed to be

$$\eta_{th} = \left(\frac{T_{t9}-T_{t0}}{T_{t4}-T_{t2}} \right) - \left(\frac{T_9-T_0}{T_{t4}-T_{t2}} \right) \quad (61)$$

For the first term, isentropic conditions state that T_{t9} equals T_{t4} because no work is done in the nozzle. Therefore

$$\frac{T_{t4}-T_{t0}}{T_{t4}-T_{t2}} = \frac{(T_{t4}-T_{t2})+(T_{t2}-T_{t0})}{T_{t4}-T_{t2}} = 1 \quad (62)$$

so that now Eq. (61) can be reduced to

$$\eta_{th} = 1 - \left(\frac{T_9-T_0}{T_{t4}-T_{t2}} \right) = 1 - \frac{T_0}{T_{t2}} \left(\frac{\frac{T_9}{T_0}-1}{\frac{T_{t4}}{T_{t2}}-1} \right) \quad (63)$$

The thermal efficiency equation is then further reduced to

$$\eta_{th} = 1 - \frac{T_0}{T_{t2}} \quad (64)$$

Using previously stated isentropic stagnation/static temperature ratios the final form of thermal efficiency for an ideal scram jet engine cycle becomes

$$\eta_T = 1 - \frac{1}{\tau_r} \quad (65)$$

Propulsive Efficiency

Propulsive efficiency is defined as the ratio of the propulsive power output versus the power input by the engine,

$$\eta_P = \frac{TV_0}{P_{engine}} \quad (66)$$

where thrust, T , is

$$T = \dot{m}_{in}(V_9 - V_0) \quad (67)$$

By substituting the engine power Eq. (56) and the thrust Eq. (67) propulsive efficiency can be denoted as

$$\eta_P = \frac{TV_0}{P_{engine}} = \frac{\dot{m}_{in}(V_9 - V_0)V_0}{\frac{\dot{m}_{in}(V_9 - V_0)(V_9 + V_0)}{2}} = \frac{2V_0}{V_9 + V_0} \quad (68)$$

From Eqs. (58) and (59), respectively the exit and freestream velocities become a square root of enthalpies, Eqs. (69) and (70).

$$V_9 = \sqrt{2(h_{t9} - h_9)} \quad (69)$$

$$V_0 = \sqrt{2(h_{t0} - h_0)} \quad (70)$$

By substituting Eqs. (69) and (70) in Eq. (68) the propulsive efficiency becomes

$$\eta_P = \frac{2\sqrt{2(h_{t0}-h_0)}}{\sqrt{2(h_{t9}-h_9)}-\sqrt{(2h_{t0}-h_0)}} \quad (71)$$

which can then be reduced to

$$\eta_P = \frac{2}{\sqrt{\frac{(h_{t9}-h_9)}{(h_{t0}-h_0)}}-1}} \quad (72)$$

Elimination of specific heat at a constant pressure, c_p , from Eq. (72) now begins to reveal the temperature ratios,

$$\eta_P = \frac{2}{\sqrt{\frac{(T_{t9}-T_9)}{(T_{t0}-T_0)}}-1}} \quad (73)$$

which can be rearranged as in Eq. (74) and used in the final form of the propulsive efficiency equation.

$$\eta_P = \frac{2}{\sqrt{\frac{T_{t9}\left(1-\frac{T_9}{T_{t9}}\right)}{T_0\left(\frac{T_{t0}}{T_0}-1\right)}-1}} \quad (74)$$

Recall that the material temperature limit to freestream temperature is

$$\tau_\lambda = \frac{T'_{max}}{T_0} \quad (75)$$

where due to isentropic assumptions no work is added from the nozzle to the exit such that

$$T'_{max} = T_9 = T_4 \quad (76)$$

thus substituting Eqs. (75) and (76) in (74) becomes

$$\eta_P = \frac{2}{\sqrt{\frac{\left(1 - \frac{T_9}{T_{t9}}\right)}{\tau_\lambda \left(\frac{T_{t0}}{T_0} - 1\right)} - 1}} \quad (77)$$

Next, using stagnation to static temperature ratios such that

$$\tau_r = \frac{T_{t0}}{T_0} = 1 + \frac{\gamma - 1}{2} M^2 \quad (78)$$

the fraction inside the square root of Eq. (77) becomes

$$\frac{1 - \frac{1}{\tau_r}}{\tau_r} = \frac{(\tau_r - 1)}{\tau_r} \frac{1}{(\tau_r - 1)} = \frac{1}{\tau_r} \quad (79)$$

Substituting Eq. (79) into Eq. (77) now results in the final form for the propulsion efficiency shown in Eq. (80).

$$\eta_P = \frac{2}{\sqrt{\tau_\lambda / \tau_r - 1}} \quad (80)$$

Overall Efficiency

Finally, overall efficiency is simply the multiplication of the thermal and propulsive efficiencies, Eqs. (65) and (80), respectively, such that

$$\eta_O = \eta_T \eta_P = \frac{2(\tau_r - 1)}{\sqrt{\tau_\lambda / \tau_r + \tau_r}} \quad (81)$$

RESULTS

So that a comparison of an ideal scramjet engine cycle analysis can be made to that of an ideal ramjet engine cycle analysis results published in chapter five of Mattingly's book, *Elements of Propulsion: Gas Turbines and Rockets*, flight conditions for the ramjet were also selected for the ideal scramjet engine. Additionally it was also assumed that the engine would experience the temperature maximum inside the engine thus the material temperature limit to freestream temperature ratio, τ_λ , was modeled after other ideal cycle analyses which state that the maximum temperature limit will be reached at the maximum material limit thus $\tau_\lambda = T_{t4}/T_0$. Later we will see what happens when the maximum temperature is experienced outside the engine.

To begin, the parametric results for constant combustion Mach numbers were obtained using ambient conditions at an altitude of 12 km. With a flight Mach number of 6, a combustion Mach number of 2, and various constants tabulated in Table 1, the ideal cycle analysis for a scramjet engine was able to be performed and the results presented in Table 3. In isolation, Table 3 demonstrates that for a scramjet engine, ideal conditions are quite favorable for generating thrust while maintaining a relatively low fuel consumption.

Table 3. Results of ideal scramjet cycle analysis parameters for a freestream Mach number of 6 and a combustion Mach number of 2 at an altitude of 12 km.

F/\dot{m}_0 [N/(kg/s)]	f	S [mg/(N-s)]	F/A_2 [N/cm ²]	η_{th}	η_p	η_o
481.93	0.03	53.57	838.30	0.88	0.88	0.77

Table 4, however, reveals the larger picture. As the freestream Mach number increases from 2 to 6 so does the overall efficiency of the scramjet from 24% to 77%. And though the ramjet shows greater efficiencies than does the scramjet over the same Mach range, the efficiencies are merely

theoretical to the point of impossible at Mach 6. At that point propulsive efficiencies for the ramjet “reaches” 103%. Also, and most notably, Table 4 shows that at Mach 3 the scramjet specific thrust of 1042.02 N/(kg/s) peaks at a magnitude almost twice the value of the ramjet specific thrust of 551.26 N/(kg/s). And though the specific thrust trends down for both engines at speeds above Mach 3 the scramjet engine still produces more specific thrust at 718.90 N/(kg/s) when flying at Mach 5 than the ramjet at its peak of Mach 3. Finally, though Mattingly did not use thrust flux as a parametric measure it is also clear that with using a modified material temperature limit to freestream temperature ratio, Eqs. (35-38), the results show that the peak for scramjet thrust could be at a much higher flight Mach number than specific thrust suggests. From the results in Table 4, the thrust flux trends upward from 18.63 N/cm² at Mach 2 to 838.30 N/cm² at Mach 6 where as specific thrust for a the scramjet peaked at Mach 3.

Table 4. Comparison of parametric measures at an altitude of 12 km for a ramjet with $M_c = 0$ and a scramjet with $M_c=2$

M_0	F/\dot{m}_0 [N/(kg/s)]		f		S [mg/(N-s)]		η_{th}		η_p		η_o		F/A_2 [N/cm ²]	
	RJ	SCRJ	RJ	SCRJ	RJ	SCRJ	RJ	SCRJ	RJ	SCRJ	RJ	SCRJ	RJ	SCRJ
2	604.26	1012.31	0.03	0.06	46.95	57.69	0.44	0.44	0.66	0.54	0.29	0.24		18.63
3	551.26	1042.02	0.02	0.05	42.23	51.16	0.64	0.64	0.76	0.63	0.49	0.40		72.16
4	383.55	917.82	0.02	0.05	42.11	50.31	0.76	0.76	0.86	0.72	0.66	0.55	n/a	214.53
5	160.15	718.90	0.01	0.04	43.65	51.49	0.83	0.83	0.95	0.80	0.79	0.67		489.89
6	-91.62	481.93	0.00	0.03	45.93	53.57	0.88	0.88	1.03	0.88	0.90	0.77		838.30

Parametric Studies Modeling Ramjet Maximum Temperature Limits

So what can be gleaned by reviewing each of the parametric measures over a range of freestream Mach numbers with different combustion Mach numbers? Figure 2 shows that though the specific thrust peaks at a flight Mach of approximately 2.5 regardless of the constant combustion Mach number the thrust per mass flow rate increases significantly as the combustion Mach number increases. For the ramjet, which is represented in Fig. 2 as having a combustion Mach of 0, it reaches a maximum specific thrust of 607.42 N/(kg/s) at Mach 2.18 and a maximum flight Mach at 5.64 but with almost no thrust. By comparison, a combustion Mach of 4 for the scramjet engine peaked at a flight Mach of 4 with a maximum specific thrust of 2024.62 N/(kg/s), over three times higher than the ramjet. Additionally the range of flight Mach from a ramjet to a scramjet increased significantly. It is clear to see that as the combustion Mach number increases the specific thrust maximum increases dramatically.

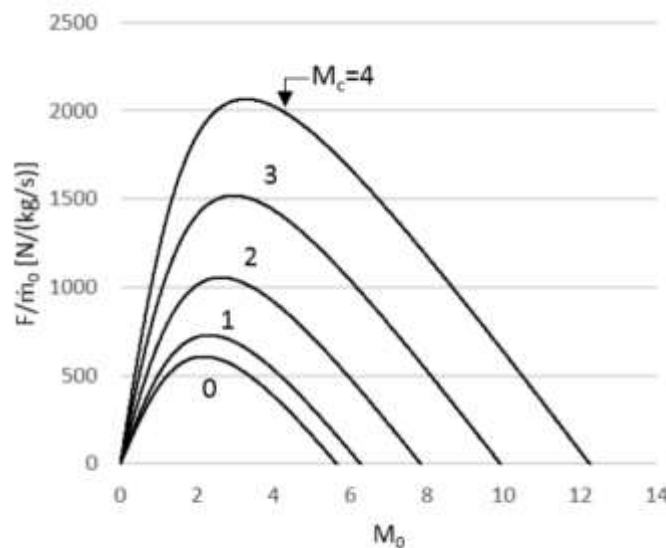


Fig. 2. Specific thrust vs freestream Mach Number of a scramjet at an altitude of 12 km as compared to a ramjet with an internal combustion $M_c = 0$

The trend in scramjet superiority of flight Mach regime continues in Fig. 3 but at a cost of fuel efficiency. Where Fig. 3 shows a maximum flight Mach range of 12.24 for the scramjet Figs. 3 and 4 show greater fuel efficiencies. The ramjet, however, pays for the increased efficiency with a loss of flight Mach range as compared to the scramjet. For both engines, however, the fuel efficiencies increase as the flight Mach number increases.

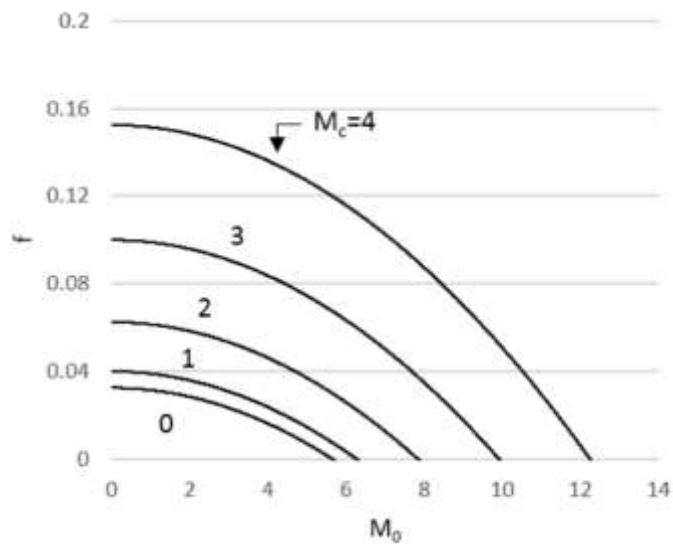


Fig. 3. Fuel-to-air mass flow ratio vs freestream Mach number of a scramjet at an altitude of 12 km as compared to a ramjet with an internal combustion $M_c = 0$

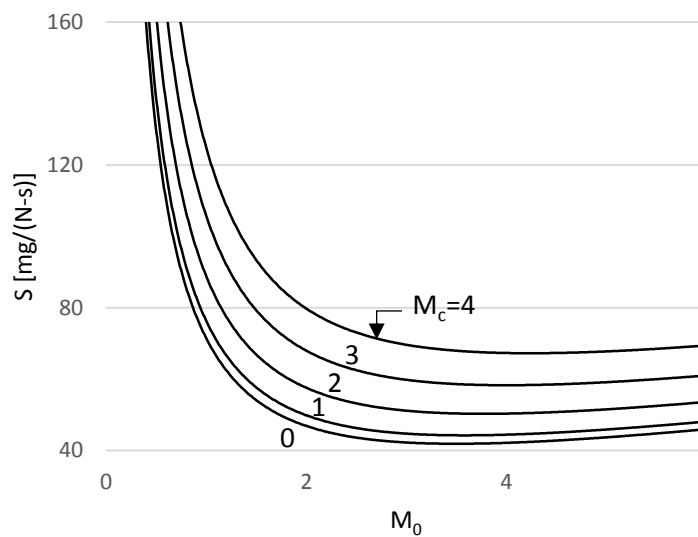


Fig. 4. Thrust specific fuel consumption vs Mach number of a scramjet at an altitude of 12 km as compared to a ramjet with an internal combustion $M_c = 0$

As we move on to the final parametric measures for this comparison study we see from Fig. 5 that since thermal efficiency is dependent only on the freestream Mach number and the ratio of specific heats the theoretical thermal efficiency is the same for both the ramjet and scramjet across all flight Mach numbers. This, however, is not the case for propulsive efficiency which also determines overall efficiency.

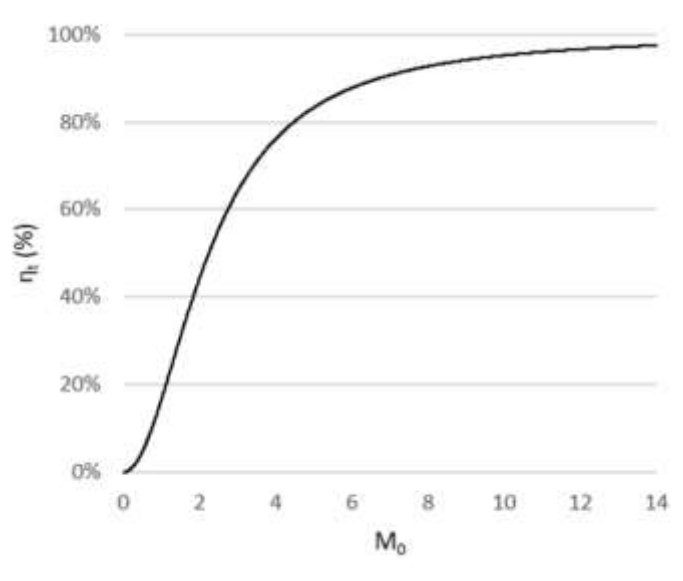


Fig. 5. Thermal efficiency vs freestream Mach number of a scramjet at an altitude of 12 km as compared to a ramjet with an internal combustion $M_c = 0$

As alluded to in previous parametric measures, the propulsive and overall efficiency of a ramjet shown in Figs. 6 and 7 as $M_c = 0$ are superior to that of the scramjet. However, as with other measures, the ramjet flight Mach range is once again limited. Ultimately though, when it comes to efficiency, regardless of the combustion Mach number the trend for propulsive and therefore overall efficiencies increases as the flight Mach number increases.

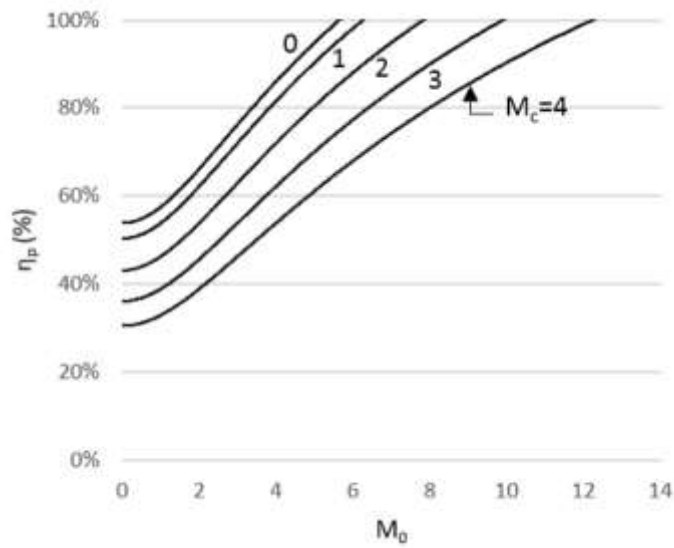


Fig. 6. Propulsive efficiency vs freestream Mach number of a scramjet at an altitude of 12 km as compared to a ramjet with an internal combustion $M_c = 0$

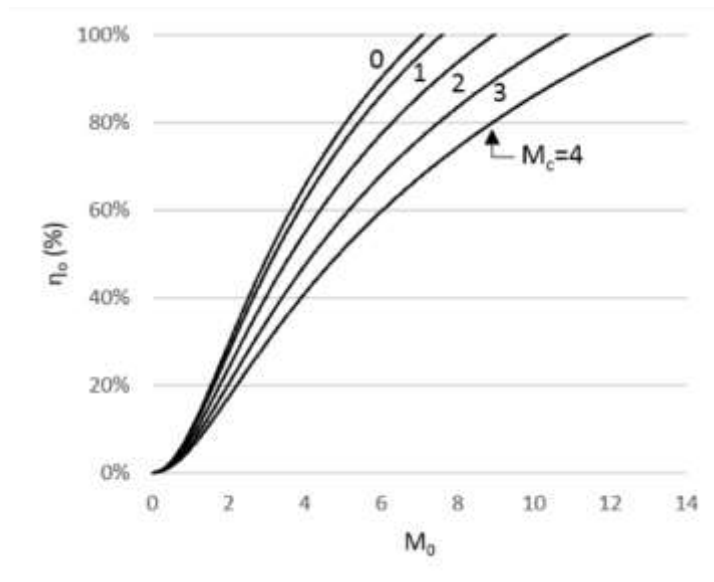


Fig. 7. Overall Efficiency vs Freestream Mach Number of a scramjet at an altitude of 12 km as compared to a ramjet with an internal combustion $M_c = 0$

Parametric Studies Modeling Material Temperature Limits When $M_c < M_0$ or $M_c \geq M_0$

For the following set of studies, attention will now be turned to how the six previously discussed parametric measures behave again using the same fuel heating value and ambient flight conditions at an altitude of 12 km as well as a seventh parameter, thrust flux. This study, however, will no longer assume that a combustion Mach number less than the flight Mach number has no effect on the parameters. Rather Eqs. (35-38) will be modeled such that when the combustion Mach is less than the flight Mach number the stagnation to static temperature ratio, T_0/T , and the total material temperature to freestream temperature ratio, τ_t , are dependent on M_c for $M_c < M_0$ and M_0 for $M_c \geq M_0$. In each case, all of the solid lines represent plausible conditions $M_c < M_0$ for the scramjet while the dotted line in the figure represents $M_c > M_0$ which is still theoretically possible. Additionally in this study, thrust-specific fuel consumption and thrust flux will be examined at different altitudes to see if the combustion Mach number or altitude has a bigger impact on fuel efficiency and thrust.

To begin, Fig. 8 shows that once again the scramjet outperforms the ramjet in both the magnitude of specific thrust and operating flight Mach range.

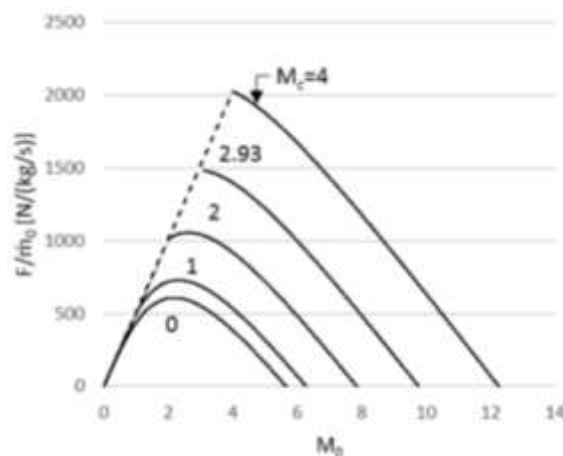


Fig. 8. Modified specific thrust vs freestream Mach number of a scramjet at an altitude of 12 km as compared to a ramjet with an internal combustion $M_c = 0$

However, the modified fuel-to-air mass flow ratio, f , shown in Fig. 9 now reaches a maximum at the dotted line, when $M_c = M_0$, at 0.13 whereas before f calculated with $M_c = 4$ almost reached a maximum of 0.16.

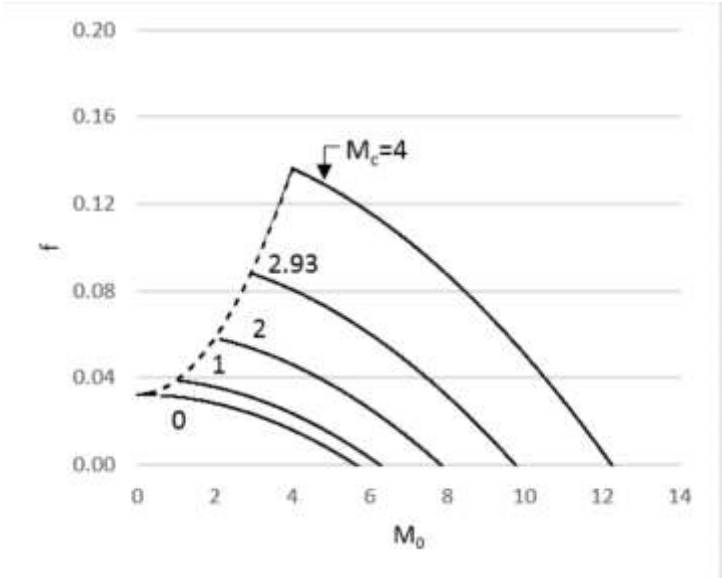


Fig. 9. Modified fuel-to-Air mass flow ratio vs freestream Mach number of a scramjet at an altitude of 12 km as compared to a ramjet with an internal combustion $M_c = 0$

Thrust-specific fuel consumption, S , once again increases as the combustion Mach number increases. Figure 10, however now shows a limit flight range for the scramjet as you increase combustion Mach. Figure 11, on the other hand, represents S a constant $M_c = 2$ over a range of altitudes. It is clear to see that M_c and not altitude influences the behavior.

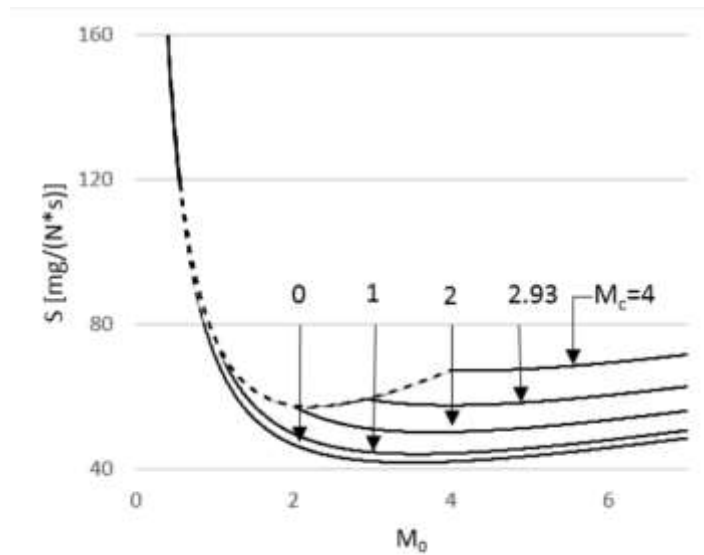


Fig. 10. Modified Thrust-Specific Fuel Consumption vs Mach Number of a scramjet at an altitude of 12 km as compared to a ramjet with an internal combustion $M_c = 0$

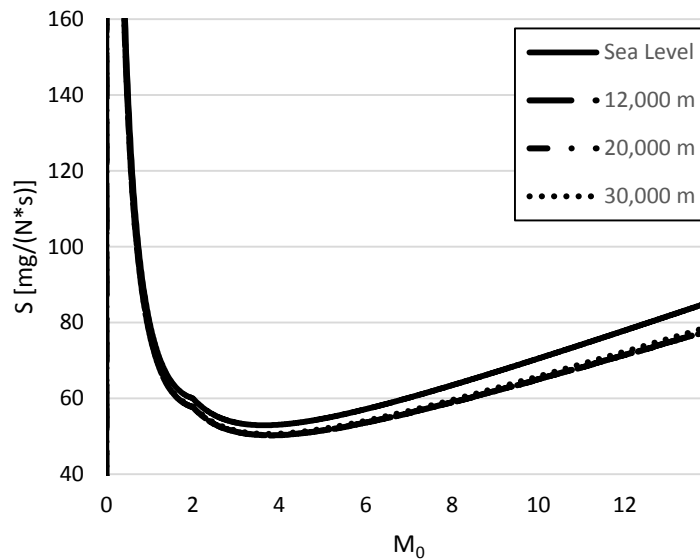


Fig. 11. Modified thrust-specific fuel consumption vs Mach number at constant combustion Mach 2 over a range of altitudes

New to the study is the thrust flux, F/A_2 . Briefly mentioned early in the results, thrust flux is a measure of the thrust force over the burner entrance area. As you can see, as the combustion Mach number increases so does the thrust flux. Where the thrust peaked at flight Mach number 4 for specific thrust a combustion Mach of 4 Fig. 12 shows a combustion Mach of only 2.93 peaking at flight Mach 9. Comparing the curved lines for $M_c = 2$ on Figs. 12 and 13 shows how

the thrust flux decreases as the altitude increases. So while the combustion Mach number has a positive effect on the thrust flux, altitude has the opposite affect though to a lesser extent.

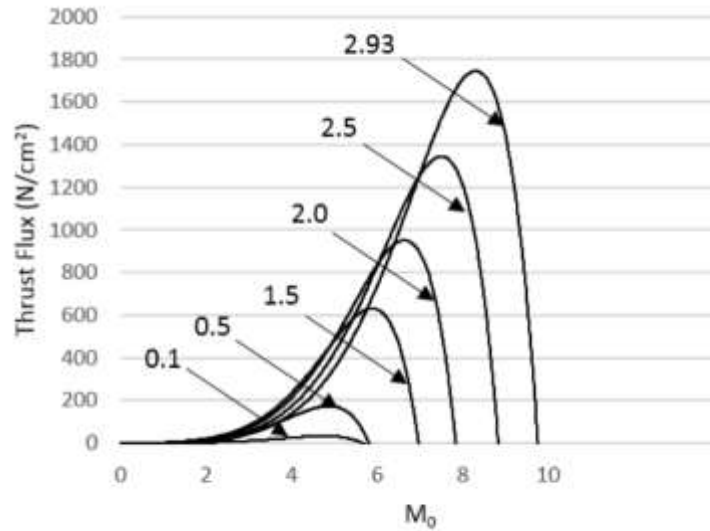


Fig. 12. Thrust flux vs Freestream Mach number of a scramjet at an altitude of 12 km

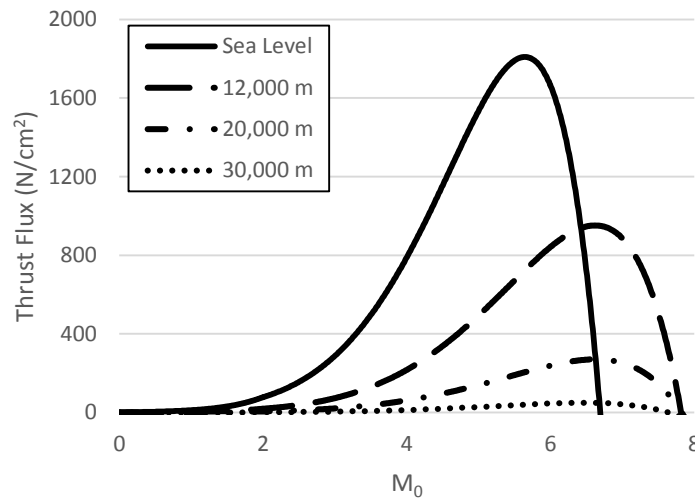


Fig. 13. Thrust flux vs freestream Mach number at constant combustion Mach 2

A review of the efficiencies is the final part of this study. As before, Fig. 14 shows that thermal efficiency is the same for both the ramjet and the scramjet. And because it is only dependent on γ and M_0 , both studies yielded identical results. As the flight Mach number increases so does the efficiency of the engine.

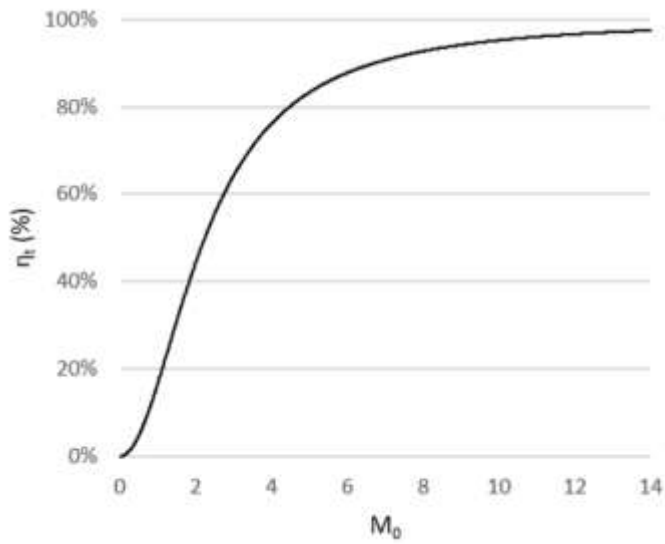


Fig. 14. Modified thermal efficiency vs freestream Mach number of a scramjet at an altitude of 12 km as compared to a ramjet with an internal combustion $M_c = 0$

Finally, just as before the ramjet propulsive and overall efficiencies shown in Figs. 15 and 16 are superior to the scramjet. However, with the examination of how $M_c < M_0$ affects the parameters there is now a lower operating limit to these efficiencies.

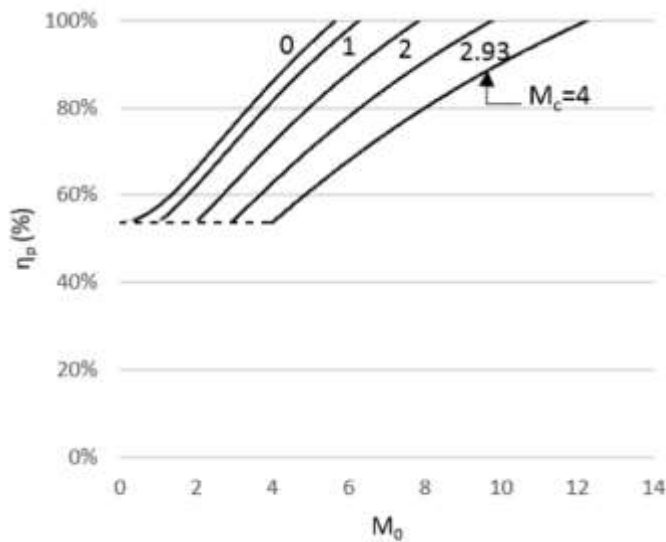


Fig. 15. Modified Propulsive Efficiency vs Freestream Mach Number of a scramjet at an altitude of 12 km as compared to a ramjet with an internal combustion $M_c = 0$

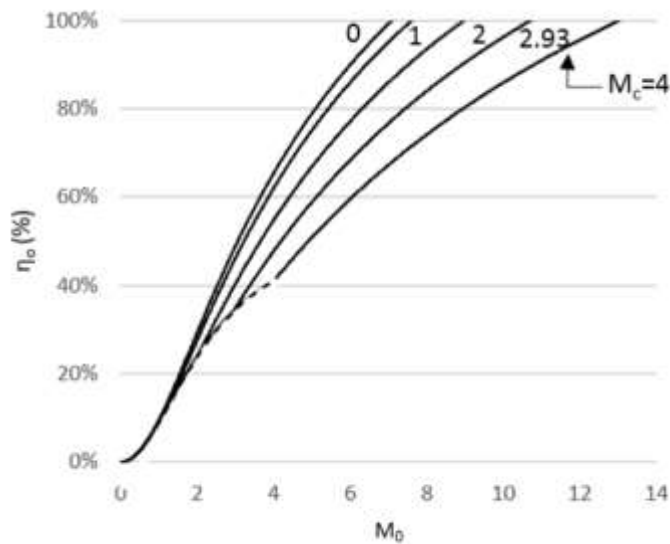


Fig. 16. Modified Overall Efficiency vs Freestream Mach Number of a scramjet at an altitude of 12 km as compared to a ramjet with an internal combustion $M_c = 0$

CONCLUSION

Though the basic design of a scramjet engine seems modest in its design, much is still unknown about the true nature of scramjet flight performance. Losses at each station due to non-ideal conditions are still difficult to model because a simple yet comprehensive set of equations to model a parametric ideal scramjet engine analysis is still being developed. To understand the scope of deriving an ideal cycle analysis for a scramjet one only needs to look at a summary of possible losses. “Most notably, the static temperature rise that is due to inefficiencies in the inlet may lead to dissociations that reduce the heat release during the combustion process” (Segal 2009). Inefficiencies such as diffuser geometry can also strongly influence loss in the diffuser which is estimated to be $r_d = 0.7$ according to author’s Hill and Peterson. Other losses include the burner and nozzle which they estimate to be $r_b = 0.95$ and $r_n = 0.98$, respectively (Hill and Peterson 1992). Losses in the combustion chamber are due to, “...mostly to friction, Rayleigh

losses, and heat transferred to the wall” (Segal 2009). Finally, additionally losses in the nozzle are reported to be, “...caused by friction, viscous dissipation in shocks, and heat lost to the structure” (Segal 2009).

Distinguishing between inefficiencies and possible false assumption about the ideal cycle analysis for a scramjet engine continues today. As recent as summer of 2016 J.A. Roux published his technical note, “Constant Velocity Combustion Parametric Ideal Scramjet Cycle Analysis,” where he comments that, “The basis for the constant velocity recommendation comes from enforcing Euler's equation across the combustor, which (because the pressure is constant) implies that the velocity will be constant across the combustor” (Roux and Tiruveedula 2016). From this paper, a constant velocity appears to model a lower, more realistic operating range for all of the parameters including thermal efficiency which decreases as the combustion Mach number increases. Additionally, the thrust flux still peaks over the same flight Mach number but at a significantly lower maximum.

Finally, the ramjet may be more efficient at lower speeds but it is clear that the scramjet outperforms the ramjet in terms of maximum thrust over a larger flight Mach regime. And while researchers still grapple with temperature limits of aircraft materials, shockwaves, geometry inefficiencies, and flow dislocations at hypersonic speeds, the pursuit of a complete parametric ideal study needs to continue so that future researchers have a foundation with which to tackle the more allusive, non-ideal solutions. Recommendations for the future include another paper on the parametric ideal scramjet engine cycle analysis but with constant velocity as well as continued literature review on engine losses.

REFERENCES

- [1] Hill, Philip G, and Peterson Carl R. "Mechanical and Thermodynamics of Propulsion." In *Mechanical and Thermodynamics of Propulsion*, by Philip G Hill, & Peterson Carl R., 155-164. Reading, Massachusetts: Addison-Wesley Publishing Company, 1992.
- [2] Lewis, Mark. "X-51 scrams into the future." *Aerospace America*, October 1, 2010: 26-31.
- [3] Mattingly, Jack D. "Elements of Propulsion: Gas Turbines and Rockets." In *Elements of Propulsion: Gas Turbines and Rockets*, by Jack D. Mattingly, edited by Joseph A. Schetz, 266-277. Reston, Virginia: American Institute of Aeronautics and Astronautics, Inc., 2006.
- [4] Musielak, Dora. "High-speed air-breathing propulsion." *Aerospace America*, December 1, 2010: 57.
- [5] Prisell, Erik G. "The Feasibility of the Scramjet; An Analysis Based on First Principles." *25th International Congress of the Aeronautical Sciences*. 2006. 1-14.
- [6] Roux, J.A, N. Shakya, and J. Choi. "Revised Parametric Ideal Scramjet Cycle Analysis." *Journal of Thermophysics and Heat Transfer* 27, no. 1 (January-March 2013): 178-182.
- [7] Roux, J.A. "Optimum Freestream Mach Number for Maximum Thrust for Ideal Ramjet/Scramjet." *Journal of Thermodynamics and Heat Transfer*, April-June 2012: 390-392.
- [8] Roux, J.A. "Parametric Ideal Scramjet Cycle Analysis." *Journal of Thermophysics and Heat Transfer* Vol. 25, no. No. 4 (October-December 2011): 581-585.
- [9] Roux, J.A. "Reply by the Author to Q. Yang, J. Chang, D. Zhang, J. Hu, and W. Bao." *Journal of Thermophysics and Heat Transfer*, 2015: 204-205.
- [10] Roux, J.A., and L.S. Tiruveedula. "Constant Velocity Combustion Parametric Ideal Scramjet Cycle Analysis." *Thermophysics and Heat Transfer* Vol. 30, no. No. 3 (July-September 2016): 697-703.
- [11] Roux, J.A., J. Choi, and N. Shakya. "Parametric Scramjet Cycle Analysis for Nonideal Mass Flow Rate." *Journal of Thermophysics and Heat Transfer* Vol. 28, no. No. 1 (January-March 2014): 166-170.
- [12] Segal, Corin. "The Scramjet Engine Processes and Characteristics." In *The Scramjet Engine Processes and Characteristics*, by Corin Segal, edited by Wei Shyy, & Michael J. Rycroft, 62-68. New York, New York: Cambridge University Press, 2009.

- [13] Smart, Michael K., Neal E. Hass, and I Allan Paull. "Flight Data Analysis of HyShot 2 Scramjet Flight Experiment." *AIAA Journal* Vol. 44, no. No. 10 (October 2006): 2366-2375.
- [14] Yang, Qingchun, Juntao Chang, Duo Zhang, Jichao Hu, and Wen Bao. "Comment on "Parametric Ideal Scramjet Cycle Analysis"." *Thermophysics and Heat Transfer*, January-March 2015: 203-204.

APPENDICES

1. Flight conditions at 12,000 m for constant combustion Mach numbers

Table 5. Parameters for light conditions at 12,000 m

Parameter	Value
a_0 [m/s]	295.0695648
h_{PR} [kJ/kg]	42,800
T_0 [K]	217
$T_{max} = T_9$ [K] (burner exit static)	1600
c_p [kJ/kg-K]	1.004
γ	1.4
R [J/kg-K]	287
P_0 [Pa] = [N/cm ²]	1.9403

Table 6. Material temperature limit conditions at 30,000 m

M_c	T'_{max} [K]	τ_λ
0	1600	7.373272
1	1920	8.847926
2	2880	13.27189
3	4480	20.64516
4	6720	30.96774

2. Flight conditions at 12,000 m for constant combustion Mach numbers where $\tau_\lambda = T'_{\max}/T_0$ for $M_c < M_0$ or $\tau_\lambda = T''_{\max}/T_0$ for $M_c < M_0$

Table 7. Material temperature limit conditions at 12,000 m when $M_c < M_0$

M_c	T'_{\max} [K]	τ_λ for $M_c < M_0$
0	1600	7.37327189
1	1920	8.84792627
2	2880	13.2718894
2.93	4347.168	20.0330323
4	6720	30.9677419

Table 8. Combustion Chamber entrance conditions at 12,000 m

$M_2=M_c$	A^*/A
0.1	0.171767333
0.5	0.746355685
1.5	0.850219361
2.0	0.592592593
2.5	0.379259259
2.93	0.252436432

Table 9. Thrust Flux variables at 12,000 m

M_c	T'_{\max}	τ_λ for $M_c < M_0$
0.1	1603.2	7.38801843
0.5	1680	7.74193548
1.5	2320	10.6912442
2.0	2880	13.2718894
2.5	3600	16.5898618
2.93	4347.168	20.0330323

3. Flight conditions at 20,000 m for constant combustion Mach numbers where $\tau_\lambda = T'_{\max}/T_0$ for $M_c < M_0$ or $\tau_\lambda = T''_{\max}/T_0$ for $M_c < M_0$

Table 10. Parameters for light conditions at 20,000 m

Parameter	Value
a_0 [m/s]	295.0724909
h_{PR} [kJ/kg]	42800
T_0 [K]	216.6543333
$T_{\max} = T_9$ [K] (burner exit static)	1600
c_p [kJ/kg-K]	1.004
γ	1.4
R [J/kg*K]	287
P_0 [Pa] = [N/cm ²]	0.547485353

Table 11. Material temperature limit conditions at 20,000 m when $M_c < M_0$

M_c	T'_{\max}	τ_λ for $M_c < M_0$
0	1600	7.38503576
1	1920	8.86204292
2	2880	13.2930644
2.93	4347.168	20.0649945
4	6720	31.0171502

Table 12. Combustion Chamber entrance conditions at 20,000 m

$M_2 = M_c$	A^*/A
0.1	0.171767333
0.5	0.746355685
1.5	0.850219361
2.0	0.592592593
2.5	0.379259259
2.93	0.252436432

Table 13. Thrust flux variables at 20,000 m

M_c	T'_{max}	τ_λ for $M_c < M_0$
0.1	1603.2	7.39980584
0.5	1680	7.75428755
1.5	2320	10.7083019
2.0	2880	13.2930644
2.5	3600	16.6163305
2.93	4347.168	20.0649945

4. Flight conditions at 30,000 m for constant combustion Mach numbers where $\tau_\lambda = T'_{max}/T_0$ for $M_c < M_0$ or $\tau_\lambda = T''_{max}/T_0$ for $M_c < M_0$

Table 14. Parameters for light conditions at 30,000 m

Parameter	Value
a_0 [m/s]	301.8025358
h_{PR} [kJ/kg]	42800
T_0 [K]	226.6499444
$T_{max} = T_9$ [K] (burner exit static)	1600
c_p [kJ/kg-K]	1.004
γ	1.4
R [J/kg-K]	287
P_0 [Pa] = [N/cm ²]	0.117188158

Table 15. Material temperature limit conditions at 30,000 m when $M_c < M_0$

M_c	T'_{max} [K]	τ_λ for $M_c < M_0$
0	1600	7.05934433
1	1920	8.4712132
2	2880	12.7068198
2.93	4347.168	19.1800974
4	6720	29.6492462

Table 16. Combustion Chamber entrance conditions at 30,000 m

$M_2 = M_c$	A^*/A
0.1	0.171767333
0.5	0.746355685
1.5	0.850219361
2.0	0.592592593
2.5	0.379259259
2.93	0.252436432

Table 17. Thrust Flux variables at 30,000 m

M_c	T'_{max}	τ_λ for $M_c < M_0$
0.1	1603.2	7.07346302
0.5	1680	7.41231155
1.5	2320	10.2360493
2.0	2880	12.7068198
2.5	3600	15.8835247
2.93	4347.168	19.1800974